

# Radiative recombination of a nonequilibrium electron-hole plasma in CdS crystals

V. G. Lysenko, V. I. Revenko, T. G. Tratas, and V. B. Timofeev

*Institute of Solid State Physics, USSR Academy of Sciences*

(Submitted August 31, 1974)

Zh. Eksp. Teor. Fiz. 68, 335-346 (January 1975)

The kinetics and shape of the spontaneous and stimulated radiative recombination spectra of an electron-hole (e-h) plasma produced by pulsed laser excitation are investigated in CdS crystals at  $T = 4.2-100^\circ\text{K}$ . The mean energy  $\langle E(n) \rangle$  per electron-hole pair, as a function of pair density, and also the position in the energy scale and shape of the e-h plasma recombination band, are calculated and found to be in satisfactory agreement with the experimental data. The "red shift" of the CdS recombination-radiation spectra observed on increase of excitation level is investigated and explained. It is demonstrated experimentally that the ground state of an electron-hole plasma in CdS crystals at helium temperatures corresponds to a density of the order of  $10^{18} \text{ cm}^{-3}$  and is 12 meV below the lowest  $A_T$  exciton term.

The spectrum of recombination radiation (RR) of CdS at sufficiently low temperatures and under conditions of intense generation of nonequilibrium carriers with the aid of an electron beam or optical pumping reveals many new properties which were hitherto attributed to various mechanisms of interaction in an exciton gas of high density. In particular, Guillaume and co-workers<sup>[1]</sup> were the first to observe a new band, called the P band, which they explained with the aid of the mechanism of radiative Auger recombination and inelastic collisions of two excitons. Somewhat later, the same point of view was developed by Mahr<sup>[2]</sup>, using as examples CdS crystals and other semiconductors of the II-VI group. It can be regarded by now as established that the appearance of the P bands at low temperatures and at a high level of nonequilibrium-carrier generation is a universal phenomenon, at least in the investigated straight-band semiconductors (see, e.g.,<sup>[3-5]</sup>).

The purpose of the present study was to investigate radiative recombination of CdS in the case of extremely high densities of nonequilibrium carriers, when the interparticle distances  $r$  are comparable with the radius  $r_B$  of the exciton Bohr orbit (i.e.,  $r_S = r/r_B = r_B^{-1}(3/4\pi n)^{1/3} \sim 1$ ). Under these conditions, as a result of screening of the Coulomb interaction, the exciton concept becomes meaningless, and the spectrum corresponds to radiative recombination of an electron-hole (e-h) plasma. The valence band and the conduction band are then filled in accordance with the given concentration of the electron-hole (e-h) pairs, and the energy spectrum itself becomes significantly restructured as a result of many-particle interactions in the system of the electrons and holes.

In Sec. 2 of the present paper we analyze the restructuring of the energy spectrum in the region of high intensities ( $r_S \sim 1$ ) and we calculate the energy of the ground state of an e-h plasma at  $T = 0$ . We report next an experimental investigation of the spectra of the spontaneous and induced radiative recombination of CdS (Sec. 3), and also the gain spectra (Sec. 4), and estimate on the basis of the experimental data the energy of the ground state of an e-h plasma. We analyze the kinetics of the spectra following pulsed excitation (Sec. 5). It is shown in particular that the P band, which was earlier attributed to exciton-exciton collisions, is the result of induced radiative recombination of a degenerate two-component plasma.

## 1. CRYSTALS AND EXPERIMENTAL TECHNIQUE

We used high-purity epitaxially grown CdS crystals 1 to 50  $\mu$  thick. The concentrations of the shallow donor and acceptor impurities, particularly those responsible for the lines of the exciton-impurity complexes on the neutral donor ( $I_2$ ) and the neutral acceptor ( $I_1$ ), did not exceed  $10^{15} \text{ cm}^{-3}$ . We present below the results obtained with one of the investigated samples, in which the donor content was at least one order of magnitude larger than the concentration of the shallow acceptor impurities (Li, Na).

The samples were placed in a cryostat with adjustable temperature in the interval  $4.2-150^\circ\text{K}$ . A temperature below  $4.2^\circ\text{K}$  (down to  $1.3^\circ\text{K}$ ) was produced by intense pumping of helium vapor.

The optical excitation of the nonequilibrium carriers was produced with a pulsed  $\text{N}_2$  laser (the power in individual pulses was 2 kW, the pulse duration and repetition frequency were respectively 10 nsec and 100 Hz). To decrease the induced recombination, the emission of the  $\text{N}_2$  laser was focused on a crystal in the form of a spot with maximum dimensions  $10 \times 10 \mu^2$ . One of the linear dimensions of the excitation region on the crystal could be controlled up to  $l \sim 0.4 \text{ mm}$  without violating at the same time the homogeneity of the excitation along  $l$ , a fact used in measurements of the gain by the methods described in<sup>[6,7]</sup>. The geometric dimensions of the exciting spot on the crystal were monitored with the aid of a measuring microscope with accuracy  $2 \mu$ .

The spontaneous-emission spectra were measured in a direction normal to the excited surface. The excited spot was projected with  $6\times$  magnification on the entrance slit of the spectrometer, and the output slit of the spectrometer, together with a special diaphragm, cut out only by the central part of the spot (approximately 2/3 of the luminous region). By the same token, this decreased considerably the contribution of the radiation from regions which were not uniformly pumped in the plane of the crystal. The spectra were analyzed with a double monochromator that ensured a spectral resolution of  $\sim 0.2 \text{ \AA}$ . We used a stroboscopic system of photoelectric registration. Smooth regulation of the delay of the strobing pulse, which had a duration  $\sim 1.5 \text{ nsec}$ , made it possible to investigate the kinetics of the recombination spectra with a time resolution of 2.5 nsec.

## 2. GROUND-STATE ENERGY OF ELECTRON-HOLE PLASMA IN CdS CRYSTALS

The principal changes that occurred with the RR spectrum of CdS at  $T = 4.2^\circ\text{K}$  and with increasing pump power from  $10^5$  to  $2 \times 10^7$   $\text{W}\cdot\text{cm}^{-2}$  are demonstrated in Fig. 1a. The chosen pump interval ensures excitation of volume concentrations of e-h pairs starting with  $n_{e,h} \sim 10^{17}$   $\text{cm}^{-3}$  and higher. The lower curve is the luminescence spectrum at a low excitation level with the aid of an ordinary mercury lamp. Figure 1 indicates the line of the exciton-impurity complexes  $I_1$  and  $I_2$  and of the free exciton ( $A_T$ ,  $\lambda = 4853.4$  Å). With increasing laser-pumping power, a new band appears on the long-wave side of the  $I_2$  line (or the M line)<sup>1</sup>. The width of this band increases with increasing volume concentration of the e-h pairs, and the "red" boundary of its spectrum experiences an appreciable shift towards lower energies.

Before we establish the connection between the observed radiation and the RR of an e-h plasma, we attempt to calculate the energy shift of the recombination spectrum of the e-h plasma, its width, and also the motion of its "violet" and "red" boundaries with changing density of the e-h pairs. To this end, following the method developed in<sup>[10, 11]</sup>, we calculated the average energy  $\langle E(n) \rangle$  per e-h pair as a function of the density of the pairs or of the dimensionless parameter  $r_S$ :

$$\langle E(n) \rangle = \langle E_{kin} \rangle + \langle E_{exch} \rangle + \langle E_{corr} \rangle, \quad (1)$$

where  $\langle E_{kin} \rangle$ ,  $\langle E_{exch} \rangle$ , and  $\langle E_{corr} \rangle$  are the average kinetic, exchange, and correlation energies. The energy is reckoned from the initial gap  $E_g$ . In the calculations we used the following parameters of CdS: electron and hole band masses  $m_e = 0.205$  and  $m_{h\perp} = 0.7m_0$ ,  $m_{h\parallel} = 5.0m_0$ <sup>[12]</sup>, state-density masses  $m_{dh} = m_{h\perp}^{2/3} m_{h\parallel}^{1/3} = 1.348m_0$ , and hole optical masses  $m_{oh} = 3(2m_{h\perp}^{-1} + m_{h\parallel}^{-1})^{-1}$

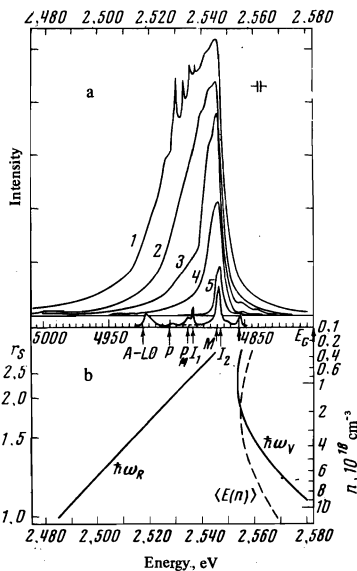


FIG. 1. a) Recombination radiation spectra of CdS at excitation power densities 16  $\text{MW}/\text{cm}^2$  (1), 5  $\text{MW}/\text{cm}^2$  (2), 1.4  $\text{MW}/\text{cm}^2$  (3), 440  $\text{kW}/\text{cm}^2$  (4), and 150  $\text{kW}/\text{cm}^2$  (5), obtained with a delay  $\tau = 12$  nsec (thermostat temperature  $T_b \sim 4.2^\circ\text{K}$ ). b) Dependence of the average energy  $\langle E(n) \rangle$  per pair of particles, and also of the "violet"  $\hbar\omega_V$  and "red"  $\hbar\omega_R$  boundaries of the recombination spectrum on the carrier density  $n$  or on the parameter  $r_S = (4\pi n/3)^{1/3} r_B$ .

$= 1.02m_0$ . The reduced exciton mass  $\mu_{ex}$ , the binding energy of the lowest  $A_T$  exciton state  $E_{ex}$ , and the radius  $r_B$  of the first Bohr orbit were respectively  $\mu_{ex} = 0.17m_0$ ,  $E_{ex} = 29.3$  meV, and  $r_B = 27.7$  Å. The dielectric constant was assumed to be  $\epsilon = 9.3$ . At  $T = 0$  we obtain for  $\langle E(n) \rangle$  in exciton Rydberg units

$$\langle E(n) \rangle = \frac{2.2}{r_S^2} - \frac{1.9}{r_S} + \langle E_{corr} \rangle. \quad (2)$$

The values of  $\langle E_{corr} \rangle$  for different  $r_S(rn)$  are:

$r_S^{-1}$ , $\text{cm}^{-3}$ :	1	1.5	2.0	2.5
$\langle E_{corr} \rangle$ , MeV:	$1.13 \cdot 10^{19}$ 22.8	$3.35 \cdot 10^{18}$ 18.7	$1.41 \cdot 10^{18}$ 16.3	$7.23 \cdot 10^{17}$ 14.6

The dependence of  $\langle E(n) \rangle$  on the dimensionless parameter  $r_S$  (or  $n$ ) is shown in Fig. 1b (dashed curve). The arrow marks here the position of the energy gap  $E_g$ .

We shall now show that the change of the width of the RR band, and also the motion of the "red"  $\hbar\omega_R$  and "violet"  $\hbar\omega_V$  boundaries of the spectrum with increasing pair density correspond to e-h plasma recombination. To do this, we recognize that the "violet" boundary at  $T = 0$  corresponds to the energy of the photons emitted upon recombination of a carrier pair directly from the Fermi surfaces of the electron and hole bands. Therefore  $\hbar\omega_V$  coincides with the chemical potential  $W$  of a system of  $N$  electron-hole pairs:

$$\hbar\omega_V = W = \frac{d}{dN} [N \langle E(n) \rangle] = \langle E(n) \rangle + n \frac{\partial \langle E(n) \rangle}{\partial n}. \quad (3)$$

If we neglect the dependence of the kinetic-energy corrections, necessitated by the interparticle interactions, on the wave vector, then the "red" boundary of the spectrum is shifted relative to  $\hbar\omega_V$  in the direction of lower energies by an amount equal to the sum of the Fermi energies of the electrons and holes:

$$\hbar\omega_R = \langle E(n) \rangle + n \frac{\partial \langle E(n) \rangle}{\partial n} - (\mu_e^0 + \mu_h^0). \quad (4)$$

Figure 1b shows together with the  $\langle E(n) \rangle$  curve also the plots of  $\hbar\omega_V$  and  $\hbar\omega_R$  against the density  $n$  (or the dimensionless parameter  $r_S$ ), calculated at  $T = 0$ .

It is seen from Figs. 1a and 1b that the calculated plots of  $\hbar\omega_V$ ,  $\hbar\omega_R$ , and  $\langle E(n) \rangle$  describe satisfactorily the positions and motion of the boundaries of the RR spectrum and its width with changing average number of the pairs of the plasma. The calculated position of the minimum of the average energy  $\langle E(n) \rangle$  at  $T = 0$ , which indeed determines the ground-state energy of the e-h plasma, corresponds to  $r_S = 2$  and  $n = 2 \times 10^{18}$   $\text{cm}^{-3}$ , and practically coincides with the position of the lowest  $A_T$  exciton term. The question of the experimental determination of the minimum of  $\langle E(n) \rangle$  will be considered in Sec. 4.

## 3. FORM OF THE SPONTANEOUS SPECTRUM OF THE RECOMBINATION RADIATION OF AN ELECTRON-HOLE PLASMA

Figure 2 shows the dependence of the form of the RR spectrum of an e-h plasma at different temperatures of the thermostat ( $T_b = 5-110^\circ\text{K}$ ) and at practically constant volume density of the pairs (the pump is fixed at  $J \sim 5 \times 10^6$   $\text{W}/\text{cm}^2$ ). We indicate first that owing to thermal dissociation there are no exciton-impurity complex lines in the spectra above  $25-30^\circ\text{K}$ . With increasing temperature, the e-h plasma emission band should broaden mainly because of the smearing of the violet part of the spectrum. This smearing corresponds to the

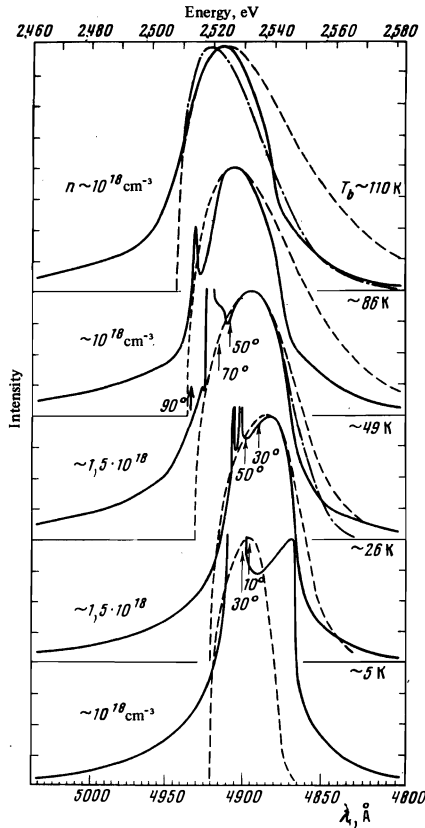


FIG. 2. Recombination-radiation spectra at thermostat temperature,  $T_b = 5-110^\circ\text{K}$ . The dash-dot and dashed lines show the approximation of the shapes of the spectra with and without allowance for reabsorption. The arrows indicate the calculated positions of the maximum of the gain at different temperatures.

temperature broadening of the distribution functions of the electrons and holes.

We have attempted to approximate the form of the spontaneous recombination spectrum of the e-h plasma with the aid of a simple model. Namely, recognizing that the interband transitions in CdS are direct ( $\mathbf{k}_e = -\mathbf{k}_h$ ), assuming the distribution of the electrons and holes to be quasi-equilibrium, and also neglecting the dependence of the matrix element of the dipole moment on the wave vector  $\mathbf{k}$ , we obtain for the form of the spontaneous spectrum

$$I_{sp}(E; \mu_{e,h}^T; T) \sim \sum_{\mathbf{k}_e = -\mathbf{k}_h = \mathbf{k}} f_e f_h \delta(E - \epsilon_e(\mathbf{k}) - \epsilon_h(\mathbf{k})). \quad (5)$$

Here  $f_{e,h} = \{1 + \exp[\epsilon_{e,h}(\mathbf{k}) - \mu_{e,h}^T]/k_0 T]\}^{-1}$  are the distribution functions of the electrons and of the holes,  $\mu_e^T$  and  $\mu_h^T$  are the chemical potentials or Fermi quasi-levels, and  $E$  is the energy reckoned from the "red" boundary of the recombination spectrum. The dispersion laws for the electrons and holes, neglecting the dependence of the corrections to the kinetic energy on  $\mathbf{k}$ , are expressed respectively in the form

$$\epsilon_e(\mathbf{k}) = \hbar^2 k^2 / 2m_e, \quad (6a)$$

$$\epsilon_h(\mathbf{k}) = \frac{\hbar^2 k^2}{2} \left( \frac{\cos^2 \theta}{m_{h\parallel}} + \frac{\sin^2 \theta}{m_{h\perp}} \right), \quad (6b)$$

where  $\theta$  is the angle between the hexagonal  $\mathbf{c}$  axis and  $\mathbf{k}$ . Further, changing over in (5) from summation over  $\mathbf{k}$  to integration, we obtain for  $I_{sp}(E; \mu_{e,h}^T; T)$ :

$$I_{sp} \sim I(E; \mu_{e,h}^T; T) = \frac{m_{h\perp} \sqrt{2E}}{\pi^2 \hbar^3} \int_0^1 \frac{1}{z^2} \left[ 1 + \exp \left\{ \frac{1}{k_0 T} \left( \frac{E}{z} \frac{m_{h\perp}}{m_e} - \mu_e^T \right) \right\} \right]^{-1} \cdot \left[ 1 + \exp \left\{ \frac{1}{k_0 T} \left[ E \left( 1 - \frac{m_{h\perp}}{m_e} \frac{1}{z} \right) - \mu_h^T \right] \right\} \right]^{-1} dy, \quad (7)$$

$$z = z(y) = 1 + \frac{m_{h\perp}}{m_e} y^2 \left( 1 - \frac{m_{h\perp}}{m_{h\parallel}} \right).$$

We note that only at  $T = 0$ , when the Fermi distributions for the electrons and holes are steplike functions,  $I(E)$  can be expressed with the aid of elementary functions. At  $T \neq 0$ , all the calculations in accordance with (7) were performed with a computer. The chemical potentials  $\mu_{e,h}^T$  were obtained with the aid of the tables for the Fermi integrals<sup>[13]</sup>.

The dashed lines in Fig. 2 represent the results of approximating the form of the spectrum with the aid of expression (7) without taking absorption into account and at the values of the parameters  $n_{e,h}$  and  $T$  indicated for each spectrum. The dash-dot curves were calculated with allowance for reabsorption and agree better with experiment. The correction for the reabsorption reduces to multiplication of expression (7) by the factor  $[1 - \exp\{-\alpha(E)\tilde{l}\}]/\alpha(E)\tilde{l}$ , where  $\tilde{l}$  is the carrier diffusion displacement length ( $\tilde{l} \sim 1.5 \mu$  in CdS) and  $\alpha(E)$  is the absorption coefficient ( $\alpha < 0$  in the case of amplification). It is seen from Fig. 2, in particular, that the role of the reabsorption increases with rising temperature, as is manifest by a noticeable narrowing of the form of the spontaneous spectrum.

On the whole, the agreement between the experimentally observed and calculated shapes of the e-h plasma spectrum at different temperatures is satisfactory. The largest discrepancies between the calculated and experimental values are observed in the region of the "red" boundary, where long-wave "tails" are observed. This is clearly seen in Fig. 3, where the e-h plasma spectra are plotted in the coordinates  $\log I$  and  $\lambda$ . The arrow in Fig. 3 indicates the "red" boundary of the spectrum. The presence of long-wave "tails" is apparently the consequence of many-particle interactions in a e-h plasma of high density. Their appearance in the recombination spectra is explained in the theoretical paper<sup>[14]</sup> as being due to interaction with plasma oscillations. Another possible explanation of the origin of the "tails" may be the mechanism of radiative Auger recombination in inelastic three-particle collisions<sup>[15]</sup>.

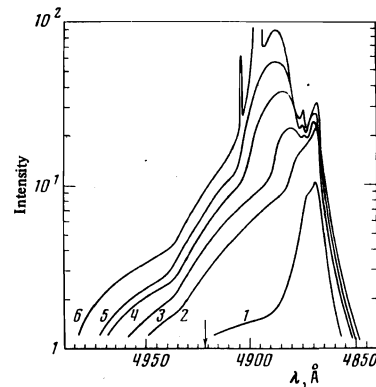


FIG. 3. Recombination-radiation spectra obtained at a power density  $\sim 3 \times 10^6 \text{ W/cm}^2$  and at different linear dimensions  $l$  of the excitation region: 1-4  $\mu$ , 2-8.6  $\mu$ , 3-13.4  $\mu$ , 4-18.2  $\mu$ , 5-23  $\mu$ , 6-27.7  $\mu$ . The observation was along the  $l$  direction.

#### 4. SPECTRAL DISTRIBUTION OF GAIN OF ELECTRON-HOLE PLASMA

A nonequilibrium and degenerate e-h plasma in straight-band semiconductors is characterized by a large gain (negative absorption) relative to radiative recombination processes. To calculate the absorption coefficient  $\alpha(\hbar\omega)$  ( $\alpha < 0$  in the case of amplification) we used the well-known expression for the rate  $r_{sp}(\hbar\omega)$  of radiative spontaneous transitions per unit volume, per unit solid angle, and per unit energy interval<sup>[16]</sup>:

$$r_{sp}(\hbar\omega) = \frac{4Ne^2\omega}{m_0^2\hbar c^3} |P|^2 I(\hbar\omega - E_g), \quad (8)$$

where  $N$  is the refractive index,  $\hbar\omega$  is the energy of the emitted photon, and  $I(\hbar\omega - E_g)$  for direct interband transitions is given by expression (7). We note that the numerical value of the square of the dipole moment  $|P|^2$  for a direct interband transition in CdS, calculated from the oscillator strength  $f$  for the  $A_{n=1}$  exciton state ( $f \sim 2 \times 10^{-3}$ <sup>[17]</sup>) is equal to  $|P|^2 = 1.6 \times 10^{-39} \text{ g}^2 \text{ cm}^2 \text{ sec}^{-2}$ . The absorption coefficient  $\alpha(\hbar\omega)$  is connected with  $r_{sp}(\hbar\omega)$  by the relation

$$\alpha(\hbar\omega) = -\frac{\pi^2 c^2 \hbar}{N^2 \omega^2} r_{sp}(\hbar\omega) \left[ 1 - \exp\left\{ \frac{\hbar\omega - E_g - \mu_e - \mu_h}{k_0 T} \right\} \right]. \quad (9)$$

Gain takes place under the condition  $\mu_e + \mu_h > 0$  and is observed in the energy interval  $\hbar\omega - E_g < \mu_e + \mu_h$ . With increasing temperature and at a fixed density of the e-h pairs in the plasma, the gains at the maximum decrease, and the spectral interval in which the gain is observed naturally becomes narrower. In particular, in the case of CdS crystals is at a pair concentration in the plasma  $n_{e,h} \lesssim 10^{18} \text{ cm}^{-3}$ , the gain disappears already at temperatures  $T \gtrsim 100^\circ \text{K}$ , as follows from calculations and experimental observations.

Figure 4 shows, for the temperatures 5 and 49°K, the gain spectra together with the RR spectra of an e-h

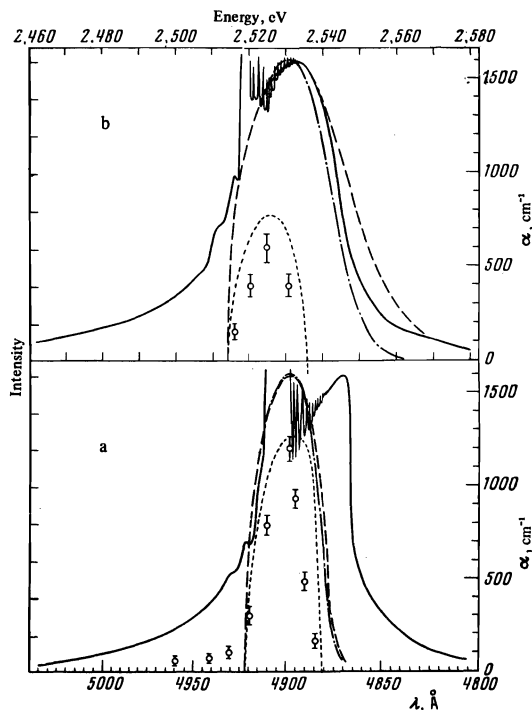


FIG. 4. Recombination radiation and amplification spectra of CdS: a)  $T_b \sim 5^\circ \text{K}$ ,  $\tau = 12 \text{ nsec}$  ( $T_e \sim 10^4 \text{K}$ ,  $n \sim 10^{18} \text{ cm}^{-3}$ ); b)  $T_b \sim 49^\circ \text{K}$ ,  $\tau = 14 \text{ nsec}$  ( $T_e \sim 50^\circ \text{K}$ ,  $n \sim 1.5 \times 10^{18} \text{ cm}^{-3}$ ).

plasma. The circles correspond to the experimental data, the dotted curve is an approximation of the shape of the gain curves with the aid of expression (9) and at values of the parameters  $n$  and  $T_e$  indicated for each spectrum in the figure caption.

It follows from Fig. 4 that at helium temperatures an e-h plasma with density  $\sim 10^{18} \text{ cm}^{-3}$  is characterized by gigantic gains ( $\alpha \gtrsim 10^3 \text{ cm}^{-1}$ ). Therefore at the maximum values of  $\alpha(\hbar\omega)$ , and if the condition  $\alpha l > 1$  is satisfied ( $l$  is the linear dimension of the excitation spot on the crystal), the IB experiences an appreciable amplification (in the presence of feedback in the system, lasing is observed). As a result, in the corresponding point of the recombination spectrum, which coincides with the maximum of the gain curve, there appear intense narrow peaks, which have a superlinear dependence on the power density and on the dimensions of the excitation region. It is important to emphasize that at helium temperatures the position of the maximum of the induced luminescence (the maximum of the gain curve) of the e-h plasma with equilibrium density  $\sim 10^{18} \text{ cm}^{-3}$  coincides with the so-called P band, which was previously connected with exciton-exciton collisions<sup>[1,2]</sup>. Thus, in our opinion, the P band is connected with induced RR of an e-h plasma.

We note in conclusion that from the gain spectra of an e-h plasma at helium temperatures it is possible to estimate experimentally the position of the minimum of the average energy  $\langle E(n) \rangle$  per particle pair. The position of the  $\langle E(n) \rangle$  minimum is determined by the "violet" boundary of the gain spectrum of the e-h plasma with equilibrium pair density  $\sim 10^{18} \text{ cm}^{-3}$ . According to our experimental observations, this minimum lies 12 MeV deeper than the lowest  $A_T$  exciton term. Thus, the experimentally observed energy of the ground state of the e-h plasma differs from the calculated one by approximately 40%.

#### 5. KINETICS OF RECOMBINATION RADIATION OF ELECTRON-HOLE PLASMA

Figure 5 shows the spectra of the spontaneous RR of CdS, obtained with different delays  $\tau$  after the start of the exciting laser pulse and at a thermostat temperature  $T_b = 4.2^\circ \text{K}$ . The oscillogram of the laser pump pulse, focused on the crystal into a spot measuring  $22 \mu$  (power density  $J \sim 3 \times 10^6 \text{ W/cm}^2$ ), is shown in the upper left corner of the figure; the origin for the oscillogram coincides with the start of the delay.

Up to delays  $\tau \sim 6 \text{ nsec}$ , the spectrum consists of one line belonging to the exciton-impurity complex  $I_2$  (M band). Starting with  $\tau \sim 8 \text{ nsec}$ , an e-h plasma band appears in the spectrum and increases in time more rapidly than M band, becoming almost comparable with it in intensity at  $\sim 12 \text{ nsec}$ . With further increase of the delay from 14 to 26 nsec, the e-h plasma and M bands decrease, remaining comparable in intensity. It is important that when the intensity of the e-h plasma band is increased by more than one order of magnitude, its width changes insignificantly. On the whole, the kinetics of the spontaneous spectrum of the e-h plasma is delayed relative to the laser pulse by approximately 2–3 nsec, whereas the time development of the  $I_2(M)$  band duplicates exactly the laser pulse.

More significant differences in the kinetics of the spectra arise under conditions corresponding to induced luminescence (or laser generation) of an e-h plasma. Figure 6 shows the wave forms of the luminescence

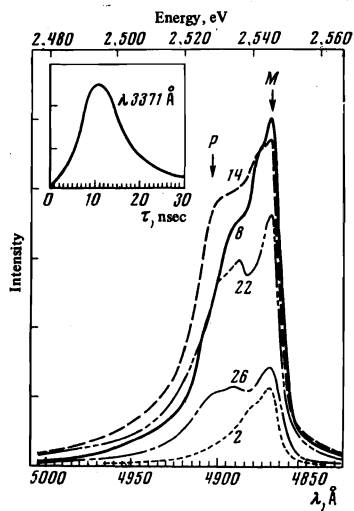


FIG. 5

FIG. 5. Kinetics of the recombination radiation spectra of an e-h plasma and of exciton-impurity complexes. The numbers at the spectra indicate the time delays in nsec.

FIG. 6. Kinetics of induced recombination of CdS in the maximum of the band of the exciton-impurity complex ( $\lambda = 4870\text{\AA}$ )—curve 1, and of an e-h plasma ( $\lambda = 4905\text{\AA}$ )—curve 2. The dashed line shows the pump pulse.  $T_b = 4.2^\circ\text{K}$ ,  $l \sim 100\mu$ .

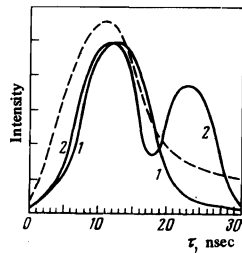


FIG. 6

spectra, obtained at the maximum of the exciton-impurity complex line ( $\lambda = 4870\text{\AA}$ ) and in the generation peak of the e-h plasma ( $\lambda = 4905\text{\AA}$ ). The dashed line in the same figure shows the waveform of the pump pulse. On the whole, the response of the luminescence of the e-h plasma duplicates the waveform of the pump pulse. At the same time, the temporal response of the recombination radiation of the e-h plasma reveals clearly the spike structure (there are two spikes on Fig. 6) so typical of the free-laser generation regime. The duration of the e-h plasma generation spikes is much shorter than the pump pulse. We note that, just as in the case of the spontaneous spectra, the kinetics of the development of the induced luminescence of the e-h plasma turns out to be delayed relative to the laser pulse by 2–3 nsec.

We emphasize that at helium temperatures and at volume-averaged pair concentrations exceeding  $10^{17}\text{ cm}^{-3}$ , the spontaneous RR spectrum of CdS always contains a band of the exciton-impurity complex besides the e-h plasma band. This indicates that regions having significantly different electron-hole densities are produced in the interior of the crystal. In spite of all the measures undertaken in our study to ensure homogeneity of the excitation, one cannot completely exclude a density gradient of the e-h pairs along the sample thickness, nor can we exclude the influence of uncontrollable defects on the surface and in the volume of the crystal. Further, at high excitation levels ( $\bar{n} \gtrsim 10^{18}\text{ cm}^{-3}$ ), generally speaking, it is immaterial where the plasma spectrum is located relative to the levels of the free electrons and of the exciton-impurity complex, for bound excited states simply do not exist in this excited volume of the crystal, owing to the screening of the Coulomb interaction. At sufficiently short recombination times in comparison with the time of establishment of the equilibrium between the e-h plasma and the crystal sections that surround it, a strongly excited layer will behave like some quasi-independent subsystem. Nevertheless, an important role is played in this case by the presence of a minimum of the free energy of the elec-

tron-hole pair  $F(n, T)$  in the given subsystem, when the e-h plasma tends to reach the equilibrium density  $n_0(T)$ . Indeed, if we hypothetically partition the e-h plasma with a certain wall, then the pressure on it will be  $P = n^2 F(n, T) / \partial n|_T$ . When the average generated carrier density is  $\bar{n} > n_0(T)$ , then  $P > 0$  and the plasma tends to increase the occupied volume. If  $\bar{n} < n_0(T)$ , the pressure becomes negative, and the plasma compresses to  $n_0(T)$ . If the  $F(n, T)$  curve has no minimum at a certain temperature, then the e-h plasma will only "spread" over the volume of the crystal, and in the spectrum of its RR we would see a band that becomes narrower and shifts on the energy scale with time<sup>[19]</sup>.

The experimentally measured delay in the appearance of the e-h plasma band (or the P band) is in our opinion precisely a characteristic of the time during which the system acquires a density  $n_0(T)$  corresponding to the minimum of the free energy<sup>2)</sup>. Further recombination takes place at a density close to  $n_0(T)$ . This is precisely why the width of the e-h plasma band changes insignificantly when the intensity at its maximum changes by one order of magnitude (Fig. 5). In other words, the recombination proceeds with practically unchanged Fermi-surfaces of the electron and hole bands.

It is quite interesting that at helium temperatures the P band appears also at relatively low densities of the e-h pairs,  $\bar{n} \sim 10^{16}\text{ cm}^{-3}$  (pump  $J \sim 10^4\text{ W/cm}^2$ ), when the Coulomb interaction is not screened. Since the minimum of the e-h plasma energy lies much deeper than the  $A_T$  exciton term, the carriers find it more profitable energywise to condense into plasmoids either as a result of collisions between the excitons or because of the presence of some condensation centers, i.e., in this sense, just as in Si and Ge crystals at low temperatures. Estimates show that the time of the binding of the excitons into a drop,  $\tau_b$ , at average concentrations  $\bar{n}_{e,h} \sim 10^{16}\text{ cm}^{-3}$ , the thermalization time  $\tau_T$ , and the radiative lifetime  $\tau_R$  are all of the same order ( $\tau_b \sim \tau_T \sim \tau_R \sim 10^{-9}\text{ sec}$ ).

The intensity and the width of the P band at low ( $J \sim 10^4\text{--}10^5\text{ W/cm}^2$ ) and fixed excitation densities depend strongly on the dimensions of the exciting spot. Since a sufficiently narrow P band (on the order of several  $\text{\AA}$ ) is observed only at relatively large linear dimensions of the excitation region on the crystal ( $l \sim 0.5\text{ mm}$ ), it can be assumed that under these conditions it is induced luminescence on a large number of electron-hole drops with an equilibrium density  $n_0 \sim 10^{18}\text{ cm}^{-3}$ , which are randomly distributed over the volume.

In conclusion, we are grateful to L. V. Keldysh and É. I. Rashba for useful discussions.

<sup>1)</sup>There is at present no meeting of minds concerning the nature of the M (and also  $P_M$ ) bands in CdS and CdSe crystals. In [9] the M band is attributed to biexciton radiation. In [9], however, there are serious arguments against the biexciton concept, and the very origin of the M and  $P_M$  bands is attributed to induced radiative decay of an exciton-impurity complex with emission of acoustic phonons.

<sup>2)</sup>A similar delay ( $\sim 0.4\text{ nsec}$ ) in the appearance of the P band was observed [18] following excitation of the luminescence of CdSe with the aid of picosecond laser pulses.

<sup>1</sup>Benoit a la Guillaume, J. Debever, and F. Salvan, Phys. Rev. **177**, 567, 1969.

<sup>2</sup>D. Magde and H. Mahr, Phys. Rev. Lett. **24**, 870, 1970.

- <sup>3</sup>R. D. Burnham, N. Holonyak, Jr., D. L. Kaune, and D. R. Seifres, *Appl. Phys. Lett.* **18**, 160, 1971.
- <sup>4</sup>J. L. Shay, W. D. Jonston, Jr., E. Buchler, and J. H. Wernick, *Phys. Rev. Lett.* **27**, 711, 1971.
- <sup>5</sup>J. L. Shay and W. D. Jonston, *Phys. Rev.* **B6**, 1605, 1972.
- <sup>6</sup>K. L. Shaklee and R. F. Leheny, *Appl. Phys. Lett.* **18**, 475, 1971.
- <sup>7</sup>L. D. Altukhov, A. F. Dite, V. I. Revenko, V. B. Timofeev, and V. M. Faĭn, *ZhETF Pis. Red.* **16**, 291 (1972) [*JETP Lett.* **16**, 204 (1972)].
- <sup>8</sup>S. Shionoya, H. Saito, E. Hanamura, and O. Akimoto, *Sol. State Comm.* **12**, 223, 1973.
- <sup>9</sup>A. F. Dite, V. I. Revenko, V. B. Timofeev, and L. D. Altukhov, *ZhETF Pis. Red.* **18**, 579 (1973) [*JETP Lett.* **18**, 341 (1973)].
- <sup>10</sup>W. F. Brinkman, T. M. Rice, P. Anderson, and S. T. Chui, *Phys. Rev. Lett.* **28**, 961, 1972. W. F. Brinkman and T. M. Rice, *Phys. Rev.* **B7**, 1508, 1973.
- <sup>11</sup>M. Combescot and P. Nozieres, *J. Phys.* **C5**, 2369, 1972.
- <sup>12</sup>D. G. Thomas and J. J. Hopfield, *Phys. Rev.* **122**, 35, 1961.
- <sup>13</sup>V. I. Fistul', *Sil'no legirovannye poluprovodniki (Strongly Doped Semiconductors)*, Nauka, 1967.
- <sup>14</sup>W. F. Brinkman and P. A. Lee, *Phys. Rev. Lett.* **31**, 237, 1973.
- <sup>15</sup>V. S. Bagaev, L. I. Paduchikh, and V. Stopachinskii, *ZhETF Pis. Red.* **15**, 508 (1972) [*JETP Lett.* **15**, 360 (1972)].
- <sup>16</sup>G. Lasher and F. Stern, *Phys. Rev.* **133**, A553, 1964.
- <sup>17</sup>S. N. Strashnikova, *Author's Abstract of Candidate's Dissertation*, Kiev, IFAN USSR (1967).
- <sup>18</sup>H. Kuroda and S. Shionoya, *Sol. State Comm.* **13**, 1195, 1973.
- <sup>19</sup>A. F. Dite, V. G. Lysenko and V. B. Timofeev, *Phys. Stat. Sol.* **66**, 9, 1974.

Translated by J. G. Adashko  
39